The Study of Cable Behavior with Two Spring-Dampers and One Viscous Damper

Nasim Shakouri Mahmoudabadi

Master of Civil Engineering, Payamnor university of Tehran, Tehran, Iran

ABSTRACT

The objective of this research was to investigate the behavior of cables with two springs-damper and one viscous damper. To this end, a major mode is adopted to control the vibration of the cable. In this mode, two damping springs are connected to both ends of the cable. The purpose is to reduce the vibrations of the cable by placing a third damper. In this case, employing spectral power density diagrams, the impact of the third damper on declining the vibration of the cable in the first three modes was presented for various values of damping coefficient for all three dampers and different damping installation places.

Keywords: *Viscous dampers, Suspension bridges, seismic response of the cable*

1. INTRODUCTION

Suspended steel cables are extensively used in modern bridges now. But, as the extents of these bridges become larger, and, thus, the length of the cables used increments, the problem of vibration in these cables becomes more visible. In some instances, it has been seen that the natural frequency of the cable agrees with the frequency of loads applied by natural forces. Thus, the phenomenon of resonance happens in these bridges. These forces are formed by wind, rain, vehicle movement on the bridge deck, or walker. If the vibration of bridge cables is not controlled by auxiliary dampers, it can cause fatigue in the cable, as well as at the junction of the bridge and the deck. The viscous damper is one of the devices that can be used to overcome the vibration of bridges. These dampers are now used in many notable bridges in the world. However, the damping applied to the cable by these dampers is limited owing to the restricted locations of these dampers, which are usually at up to 5% of the cable length from the end of the path. Hence, it is quite important to reach maximum damping in the cable by devising fitting dampers. These include the Breton Bridge in France, the Sunshine Skyway Bridge in Florida, and the Aristotle Bridge in Japan. Nevertheless, the design of these dampers has been done empirically working experiments like wind tunnels. Accordingly, it is necessary to be able to create methods for the design of these dampers without the cost of numerical analysis techniques. In this project, such methods were studied.

The design methods of viscous dampers have been reviewed by various authors. In 2001, Main and Jones (2001) managed to reach an approximate equation for the curve suggested by Pachecco by analytically solving the motion equation governing the cable, and adopting some simplifying premises such as the closeness of the damper to the end of the cable. They also studied the effect of the damper when it is at a substantial distance from the end of the cable in (Main and Jones, 2002) by examining the analytical solution of the equation governing

cable movement. According to their research, as the distance of damper to the end of the cable increases, different behavioral regimes appear in the cable's behavior, and new oscillating modes arise in the cable. Overall, they were able to list three types of behavioral regimes for moving cables. In 2003, Main and Jones recognized the effect of hardness on the damper. This mode is considered by modeling a spring with a linear hardness attached to the damper. They settled that when the damper has a hardness, the hardness effect can be modeled by decreasing the distance of the damper with the end of the cable. In fact, they came up with an equation to obtain an effective damping location with hardness. The solution methods of all the cited authors were based on the finite series method. Furthermore, all these authors considered the vibration behavior of the cable as linear. Another detail is that all the authors have examined the case where only one damper connected to the cable. The modeling of the cable's elements was done by the finite element method by some authors in the past. For illustration, one can refer to references (Ozdemir, 1979; Jayaraman AND Knudson, 1981; Wang et al., 1998; Ni et al., 2002). The benefit of the finite element method is that the effect of attaching the dampers and the spring to the cable can be easily taken into account by joining the damping coefficient in the total damping matrix and the spring stiffness coefficient in the total cable stiffness matrix. So far, few authors have studied the nonlinear behavior of cables owing to considerable deformations. For instance, YU and XU in 1999 modeled the cable motion nonlinearly employing the finite difference method.

It is clear that the vibration status of the cable, when two or three dampers are connected to it, has not been examined so far, which is examined in this research.

2. MATERIALS AND METHODS

Cable treatment with a linear viscous damper
By neglecting the flexural stiffness of the cable and assuming linear behavior, the differential equation dictating the movement of the cable is:

$$T \frac{\partial^2 v}{\partial x^2} = m \frac{\partial^2 v}{\partial t^2} + c \frac{\partial v}{\partial t} \delta(x - x_c) \qquad (1)$$

Using the Galerkin's method and using $\phi_{0i}(x)$ functions as weight functions, applying the orthogonality feature, we have:

$$\int_0^L \phi_{0i}(x) \phi_{0j}(x) dx = \frac{1}{2} L \delta_{ij} \qquad (4)$$

Where δ_{ij} is the Cronker Delta function. Thus, Equation (1) becomes the following matrix:

$$Mb'' + Cb' + Kb = \{0\} \qquad (5)$$

Where:

Equation (7) involves dimensionless cable and damper parameters.

$$M_{ij} = \delta_{IJ} \qquad (6)$$

$$C_{ij} = 2 \left[\frac{c}{mL\omega_{01}} \right] \sin\left(\frac{\pi i x}{L} \right) \sin\left(\frac{\pi j x_c}{L} \right) \qquad (7)$$

Practical span of cable and damper values

i , x_c / L , $\dfrac{c}{mL\omega_{01}}$ are independent from one another.

Due to administrative issues, the damper can only be linked to the end of the cable.

$$y(x) = \begin{cases} a_k \dfrac{\sin(\beta x)}{\sin(\beta x_k)} & , \quad 0 \le x \le x_k \\[3mm] a_k \left[\cos(\beta x'') - \dfrac{\sin(\beta x'')}{\tan(\beta x_c'')} \right] + a_c \dfrac{\sin(\beta x'')}{\sin(\beta x_c'')} & , \quad x_k \le x \le x_c \\[3mm] a_c \dfrac{\sin(\beta x')}{\sin(\beta x_c')} & , \quad x_c \le x \le L \end{cases} \qquad (11)$$

Where a_c, a_k respectively indicate the size of the spring and damper. In general, they are complex and induce the phase difference between the two points.

$$K = \frac{(k / \beta T)\left[1 + \cot^2(\beta x_c)\right]}{\left[1 + \cot^2(\beta x_k)\right] + (k / \beta T)\left[\cot(\beta x_k) - \cot(\beta x_c)\right]} \qquad (12)$$

If k=0, then K=0 and the equation is imaginary. While the term on the right is complex in general. Hence, by zeroing the real part, an equation is reached to determine the specific

In most cases, the product of two values, i, xc / L, is less than 15%.

Further, the real range of the $\dfrac{c}{m.L.\omega_{01}}$ is known and practically there is no need to consider much great values for *c*. Because in this case, it is as if where the damper is, a support is placed. Thus the modal attenuation ratio will tend to zero once more. Because the existence of this support will not allow energy loss by the cable.

Cable behavior with a single spring-damper system
As in (Wang et al., 1998), the impact of the spring or the existence of stiffness in the damper can be displayed as the reduction of the distance of the damper from the end of the cable.
Assuming low intrinsic damping and ignoring the flexural stiffness, the differential equation ruling the cable can be written as:

$$m\ddot{y} = Ty'' \qquad (8)$$

The balance of forces where the spring and the damper join as follows:

$$T\left[y'(x_k^+) - y'(x_k^-)\right] = ky(x_c) \qquad (9)$$

$$T\left[y'(x_c^+) - y'(x_c^-)\right] = c\dot{y}(x_c) \qquad (10)$$

Zero displacement boundary conditions must likewise be met at the ends of the cable, and the cable displacement must be constant at the intersection of the spring and the damper.

The answer to the equation with boundary conditions and continuity is:

In (9), *K* represents the effect of the spring, and is defined as:

frequencies that are independent of the damping coefficients *c*. This equation can be reformulated as:

$$\tan(\beta L) = \frac{(i\eta + K)\sin^2(\beta x_c)}{1 + (i\eta + K)\sin(\beta x_c)\cos(\beta x_c)} \quad (13)$$

Where:

$$\eta = \frac{c}{\sqrt{Tm}} \quad , \quad \chi = \frac{kx_k}{T} \quad (14)$$

Further, the complex frequencies are can be written as:

$$\omega_n = n + \Delta\omega_n \quad (15)$$

The effective placement of the damper, x_c^{eff}, is:

$$x_c^{eff} = x_c \frac{[1 + \chi(1 - x_k / x_c)]}{(1 + \chi)} \quad (16)$$

For the special condition where the spring and damper are at the same point, Equation (12) is rewritten as:

$$\sin(\beta L) + \left(\frac{k}{\beta T} + i\frac{c}{\sqrt{Tm}}\right)\sin(\beta x_c)\sin(\beta x_c') \quad (17)$$

In this case, we have:

$$x_c^{eff} = \frac{x_c}{(1 + \chi)} \quad (18)$$

Therefore, the effect of the spring is like reducing the effective location of the damper.

Study and analysis of the equation of free vibration of the cable with a damper Problem formulation

The goal of this section is to investigate the behavior of the cable in general to provide an analytical solution to the free vibration equation of the cable. The system under study is presented in Figure (1).
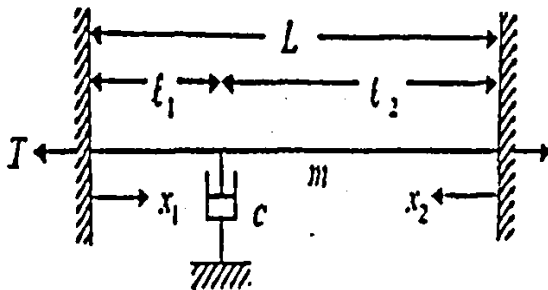

Figure 1. The studied system

It is seen that the damper is split into two parts in which, l2≥l1. Considering that the tension in the cable is great compared to its weight, the natural flexural stiffness and damping of the cable are neglected. In fact, the cable is assumed to be straight and

with no curvature. In this case, the resulting equation is established in each part of the cable:

$$m\frac{\partial^2 y_k(x_k,t)}{\partial t^2} = T\frac{\partial^2 y_k(x_k,t)}{\partial x_k^2} \quad (19)$$

Where $y_k(x_k,t)$ is the lateral rise and x_k is the coordinates in the direction of the cable in the k-th part of the cable. m is the mass of the unit length, and T is the tension in the cable. This equation is accurate in all parts of the cable but the damper attachment point. At this point, the boundary conditions for the continuation of cable relocation and balance of power must be met. Consider that dimensionless time is specified as:

$$\tau = \omega_{01}t \quad (20)$$

Where:

$$\omega_{01} = (\pi / L)\sqrt{T / m} \quad (21)$$

To solve Equation (19) by counting the boundary conditions, continuity, and equilibrium, the solution function is considered in the following separate form:

$$y_k(x_k,\tau) = Y_k(x_k)e^{\lambda l} \quad (22)$$

Where λ is a dimensionless eigenvalue that is generally a complex number. In cases where the damping ratio is relatively large, most of the magnitude λ is related to its real part. In more detail, as the damping ratio raises, λ tends to a real number. By putting Equation (22) in Equation (19), the resulting ordinary differential equation is obtained:

$$\frac{d^2 Y_k(x_k)}{dx_k^2} = \left(\frac{\pi\lambda}{L}\right)^2 Y_k(x_k) \quad (23)$$

Since λ is a complex number, the solution of Equation (23), which actually gives the form of cable modes, will also be complex. The continuity of displacement at the damper and the boundary conditions of displacement at the ends of the cable can be met by holding that Equation (23) is solved as:

$$Y_k(x_k,\tau) = \gamma\frac{\sinh(\pi\lambda x_k / L)}{\sinh(\pi\lambda l_k / L)} \quad (24)$$

Where γ is the solution at the damper location. The equilibrium equation at the damper position can be formulated as:

$$T\left(-\left.\frac{\partial y_2}{\partial x_2}\right|_{x_2=l_2} \quad -\left.\frac{\partial y_1}{\partial x_1}\right|_{x_1=l_1}\right)=\left.c\frac{\partial y_1}{\partial r}\right|_{x_1=l_1} \quad (25)$$

Where c is the damping coefficient of the damper. Differentiating the form the solution declared in Equations (22) and (24) and putting it in Equation (25), we obtain the following equation:

$$\coth(\pi\lambda l_1/L)+\coth(\pi\lambda l_2/L)+\frac{c}{\sqrt{Tm}}=0 \quad (26)$$

Equation (26) is known as the frequency equation. For the special values $c/\sqrt{Tm}$ and l_1/L, Equation (26) can be solved

$$\sin(2\pi\varphi l_1/L)\cosh(2\pi\sigma l_2/L)+\sin(2\pi\varphi l_2/L)\cosh(2\pi\sigma l_1/L)=\sin(2\pi\varphi) \quad (28)$$

This Equation is independent of $c/\sqrt{Tm}$ and its branches of solving gives the separate λ values for a given l_1/L value. Accordingly, the permissible damping ratio values with the corresponding oscillating frequencies can be reached. Equation (28) is named the phase equation. While the solution branches

$$\frac{\sinh(2\pi\sigma l_1/L)}{\cosh(2\pi\sigma l_1/L)-\cos(2\pi\varphi l_1/L)}+\frac{\sinh(2\pi\sigma l_2/L)}{\cosh(2\pi\sigma l_2/L)-\cos(2\pi\varphi l_2/L)}+\frac{c}{\sqrt{Tm}}=0 \quad (29)$$

For a given value of λ with real and imaginary parts σ and φ satisfying Equation (27), the corresponding $c/\sqrt{Tm}$ value can be achieved from (28). Equation (24) to calculate the shape

$$Y_k(x_k)=A_k\left[\sinh(\pi\sigma x_k/L)\cos(\pi\varphi x_k/L)+j\cosh(\pi\sigma x_k/L)\sin(\pi\varphi x_k/L)\right] \quad (30)$$

Where the complex coefficients are denoted by A_k and are calculated by the following equation:

$$A_k=y/\sinh(\pi\lambda l_k/L) \quad (31)$$

Three types of behavior can be regarded for the solution. The first is the decreasing non-oscillating behavior (corresponding to φ = 0), which is equal to a state named supercritical damping. Three types of behavior can be regarded for the solution. The first is the decreasing non-oscillating behavior (corresponding to φ = 0), which is equal to a state named supercritical damping. The other is the non-reducing oscillating behavior (σ = 0) equivalent to the zero damping state, and the last is where the damping directs towards the critical damping $(\xi\rightarrow 1 \quad, \quad \sigma\rightarrow\infty)$.

For nonlinear analysis of cables and also in cases where the cable is attached to a damper, Newton-Raphson and Newmark methods are used.

Analysis of nonlinear systems by Newmark method

immediately numerically to achieve the damping ratio in any coveted mode. Each special value can be formulated as a combination of real and imaginary parts as:

$$\lambda_i=\frac{\omega_i}{\omega_{01}}\left(-\xi_i+j\sqrt{1-\xi_i^2}\right) \quad (27)$$

Where ξ is the damping ratio and ω_i is the quasi-nondamping natural frequency.

By expanding Equation (27) and separating the imaginary and real parts, after simplification, the resulting equation is obtained:

of Equation (27) are symmetric revolving the σ = 0 axis, only the negative values of σ are counted here. Because positive σ values correspond to negative $c/\sqrt{Tm}$ values, which does not make sense physically. Considering the real part of Equation (27), after simplification, the resulting equation is obtained:

of modes can be implicitly expanded into imaginary and real expressions to reach this equation:

The Newmark equation displayed in the previous part for linear systems can also be used for nonlinear analysis. repetition methods can be used to eliminate the computational error. The key equation that is solved at each time step for nonlinear systems is as:

$$\left[\dot{K}_T\right]\{\Delta U\}=\{\Delta\dot{P}\} \quad (32)$$

Where:

$$\left[\dot{K}_T\right]=\left[K_T\right]+\frac{\gamma}{\beta\Delta t}\left[C\right]+\frac{1}{\beta(\Delta t)^2}\left[M\right] \quad (33)$$

Where $[K_T]$ is the tangential stiffness matrix of the structure. In the following section, its formulation for the cable element will be given. This equation is nonlinear. Because the tangential stiffness $[K_T]$ depends on the displacement vector {U}. Currently, the iteration method is described following Figure (1).
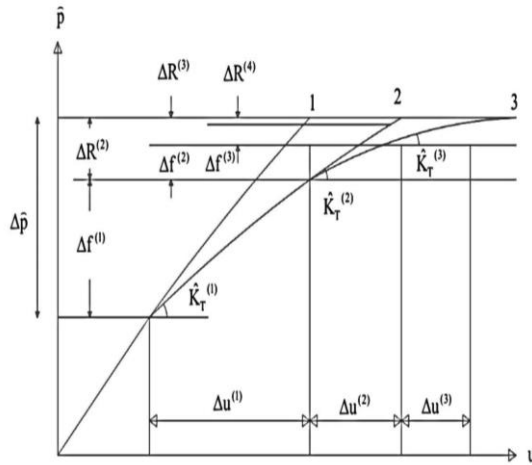
Figure 2. Newton-Raphson iteration method in a time step (Figure from (Çakmak, 1996))

The first iterative step is to apply Equation (32) to the method described above:

$$\left[\hat{K}_T\right]\left\{\Delta U^{(1)}\right\} = \left\{\Delta\hat{P}\right\} \tag{34}$$

To determine $\{\Delta U^{(1)}\}$, which is the first approximation for the final value $\{\Delta U\}$, the following steps are followed. Corresponding to the dislocation $\{\Delta U^{(1)}\}$ exists the real force $\{\Delta f^{(1)}\}$ which is lower than $\left\{\Delta\dot{P}\right\}$. Accordingly, the residual force is:

$$\left\{\Delta R^{(2)}\right\} = \left\{\Delta\hat{P}\right\} - \left\{\Delta f^{(1)}\right\} \tag{35}$$

The additional dislocation $\left\{\Delta U^{(2)}\right\}$ due to the residual force is:

$$\left[\dot{K}_T\right]\left\{\Delta U^{(2)}\right\} = \left\{\Delta R^{(2)}\right\} - \left\{\Delta\hat{P}\right\} - \left\{\Delta f^{(1)}\right\} \tag{36}$$

This additional displacement is used to determine a new value for the residual force, and the process keeps going until convergence is obtained. Note that in each iteration in relation (36), the Tangential stiffness matrix $\left[\dot{K}_T\right]$ also should be updated.

The iteration process ends after I iterations, when the developmental displacement of $\{\Delta U^{(1)}\}$ is very small compared to $\left\{\Delta U\right\} = \sum_{J=1}^{r}\left\{\Delta U^{(J)}\right\}$. That is:

$$\frac{\left\|\left\{\Delta U^{(1)}\right\}\right\|}{\left\{\Delta U\right\}} \leq \varepsilon \tag{37}$$

Thus, the evolution of displacement from the time step i to i + 1 is reached from the following equation:

$$\left\{\Delta U\right\} = \sum_{j=1}^{i}\left[\left\{\Delta U^{(j)}\right\}\right] \tag{38}$$

With the known $\{\Delta U_i\}$, the calculation is as before. It is worth mentioning that in the computer program used, the permissible error rate ε equals 0.01.

Calculation of the tangential stiffness matrix for the cable element

As can be seen, to solve the dynamic problem by Newton-Raphson method, it is needed to know the tangential stiffness matrix. Overall, this matrix is different from the element hardness matrix specified in Chapter 4. In fact, if the displacement vector is denoted by $\{U\}$, the following relation should hold for the tangential stiffness matrix $[K_r]_I$ in the i-th time step and the cable stiffness matrix $[K]$ in the time steps i and i+1:

$$\left[K_{i+1}\right]\left\{U_{i+1}\right\} = \left[K_i\right]\left\{U_i\right\} + \left[K_T\right]_i\left\{\Delta U_i\right\} \tag{39}$$

$$\left\{\Delta U\right\} = \left\{U_{i+1}\right\} - \left\{U_i\right\} \tag{40}$$

Hence, if a relation can be specified as follows (which, as seen, is the case with the cable element),

$$\left\{Fi(\{U\})\right\} = \left[K(\{U\})\right]\{U\} = \left(\left[K_0\right] + \left[K_1\right] + \left[K_2\right]\right)\{U\} \tag{41}$$

Then by differentiating {Fi ({U})}, the following equation is achieved:

$$\left\{dF_i(\{U\})\right\} = \left[K_T\right]\left\{dU\right\} \tag{42}$$

For the cable element, this is done, and ultimately, the element stiffness matrix $[K_T]_J$ is obtained as follows:

$$\left[K_T\right]_J = \left[K_{T1}\right]_J + \left[K_{T2}\right]_J \tag{43}$$

Where:

$$\left[K_{T1}\right]_J = \left[K_{0J}\right] + \left[K_{1J}\right] + \left[K_{2J}\right] \tag{44}$$

And:

$$\left[K_{T2}\right]_J = \left[K_{2J}\right] + EAJ\int_{-1}^{2}\left[B_0\right]^T\left[B_1\right]d\xi + \frac{EA}{J}\int_{-1}^{+1}\left[\left(\left[B_0\right] + \left[B_1\right]\right)\left\{U_j\right\}\right]\left[N'\right]^T\left[N'\right]d\xi \tag{45}$$

Where $[K_{0J}]$, $[K_{1J}]$, and $[K_{2J}]$ are respectively the first-, second-, and third-degree stiffness matrices and are determinable.

3. RESULTS AND FINDINGS

Specifications of the used cable

In all cases discussed in this chapter, a cable with the specifications of Table (1) has been used:

Table 1. Specifications of the cable used

T(N)	m(kg/m)	E(Mpa)	A_S	Length
10000	6	$2/10x10^5$	177	20

In this Table, A_S is the cross section of the cable, E is the modulus of elasticity, m is the mass per unit length, and T is the tensile force of the cable. The first vibration frequency of such a cable is 1.02 Hz, which agrees with the first vibration frequency of a real-scale suspension bridge cable, usually between 1 and 3 Hz. Additionally, for cable modeling, 50 three-node cable elements of equal length have been employed. The curvature of the cable is neglected, and the cable is modeled directly. In cases where the cable is subjected to external stimulation, the damping matrix of the cable is considered according to the Riley model in proportion to the mass matrix and its initial stiffness matrix. That is:

$$[C] = \alpha[M] + \beta[K] \tag{46}$$

The coefficients α and β are chosen so that the damping ratio of the first two vibration modes of the cable equals 0.15%. For a cable specified as in Table (1), α and β are respectively 0.0128 and $1.56*10^{-4}$. The damping ratio of the cable has been neglected for the parts where the cable is analyzed for specific values.

Cable behavior with the two-spring -dampers and one viscous damper

The system studied here is a cable with two springs-damper and one extra viscous damper as in Figure (4). In practice, this system is used when the vibrations, despite the placement of two springs-dampers, is still considerable. The question is, "What should be the attenuation coefficient of the third damper for a given junction so that vibrations are reduced to the desired level?" That is, it is desirable to learn how much vibration energy the third damper can dissipate. The significance of this question becomes clearer with the next example. Suppose a cable with the characteristics in Table (1) is excited with a sine excitation function with a variable frequency of 0.5 to 10 Hz for 120 seconds. Suppose that the place of application of the load is 15% of the length of the cable from its end and its magnitude is 10 Newtons. Also, assume that the two dampers employed have the same damping coefficient and are chosen to receive the maximum damping ratio in the first vibration mode. Also, it is assumed that these two dampers have no stiffness. For a cable with the specs of Table (1), for the connection of two springs-dampers at 4% of the cable length, the damping coefficient of springs-dampers is 1900 N.s / m. Also, consider that the installation position of the viscous damper at 6% of the cable length and its damping coefficient is equal to the damping coefficient of the other two springs-dampers. To achieve an appropriate measure of the ability of the third damper to dissipate the vibration energy of the cable, the Power Spectrum Density (PSD) diagram is determined at all nodes, and the average spectrum received from all nodes is recorded as the average PSD. The resulting diagram is displayed in Figure (5). This figure further shows the average PSD curve for comparison with only two springs-dampers attached to the cable.

According to the figure, when the damping coefficient of the third damper is equal to two springs-dampers, in the first mode it reduces by 13% and in the second mode by 5% of the vibration energy compared to the connection state of the two springs-dampers alone. In contrast, 2.5% adds to the energy of the mode in the third mode and 17% in the fourth mode. It is obvious from this case that the addition of a third damper may harm the damping ratio of the cable in some modes.
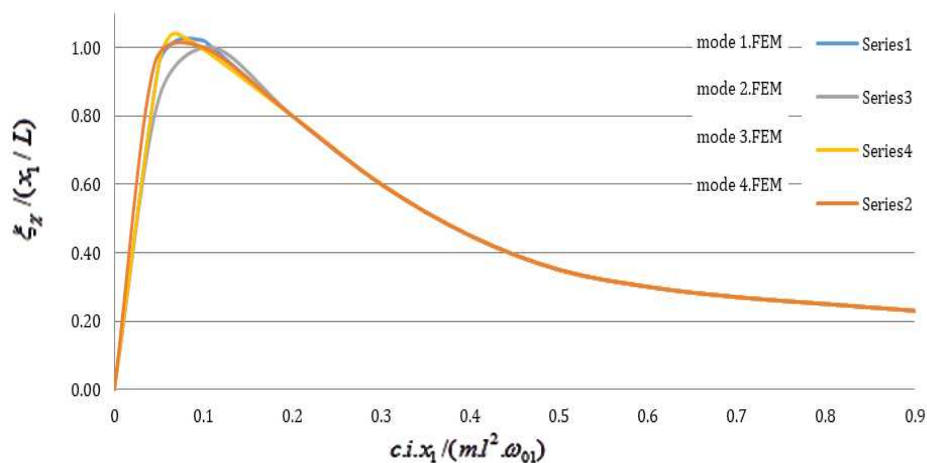

Figure 3. Damping ratio curve in which the two dampers-springs are connected at x_1/L=0.04 or χ=1.
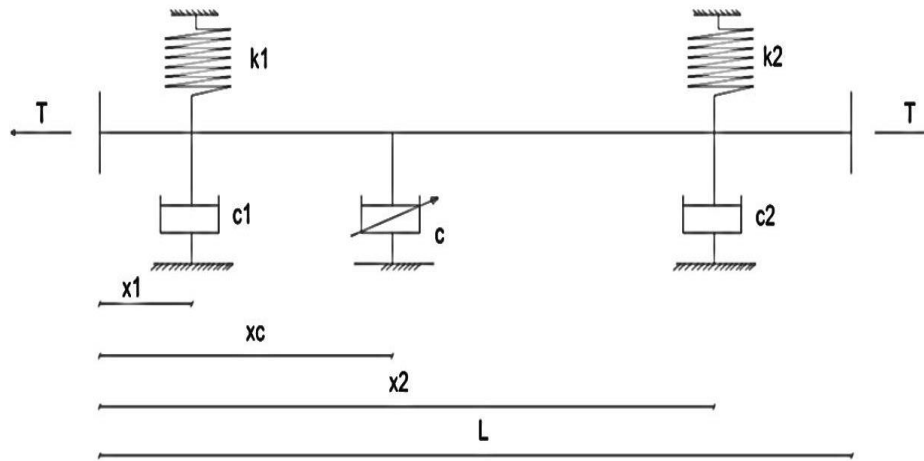
Figure 4. Cable with two dampers-springs and a viscous damper
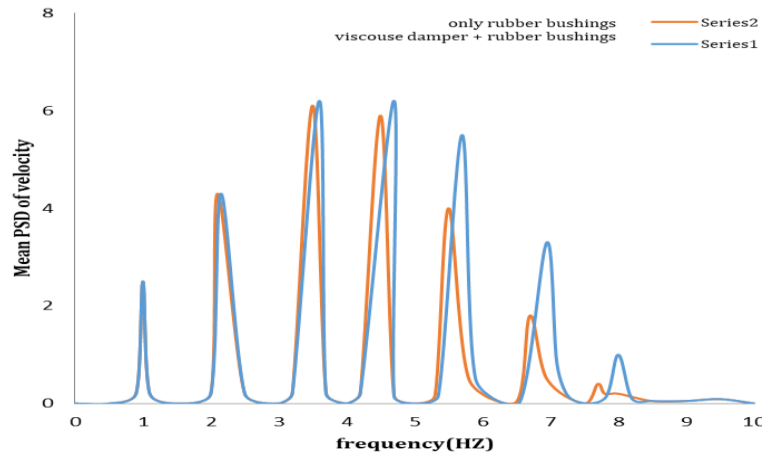

Figure 5. Comparison of the average PSD with and without the installation of the third viscous damper. (Springs-dampers are connected at 4% of the cable length and the third damper is connected at 6% of the cable length and c1 = c2 = c3 = 1900N.s / m)

To explain the cause of this happening, two limit states can be pictured for the third damper. The first case is the cable without In the second case, the third damper has an infinite damping coefficient. That is $C_3 \rightarrow \infty$, this state is presented in Figure (6).
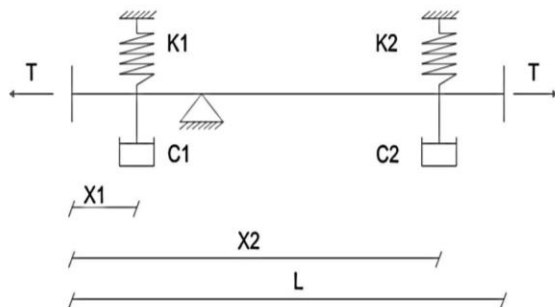

Figure 6. Cable with two springs-dampers and infinite coefficient of the third damper

the third damper (Figure (5)). In this case, the c3 / c1 ratio equals zero.

In this instance, the third damper locks the cable at the joint, and therefore effectively the spring-damper on the left will not perform a role in decreasing vibrations, and thus, the damping ratio of the cable is reduced.

After seeing the above limit, it is assumed that the installation of a third attenuator, as presented in Figure (5), may decrease the damping ratio of the cable in some of its modes. Thus, in this section, we have tried to achieve suitable curves for the design of the third damper by performing sensitivity analysis like what was seen in the earlier example.

To study the sensitivity in this section, a cable with the specifications of Table (1) is excited with a sine function with a variable frequency of 0.5 to 10 Hz at 15% of the cable length from the end with a magnitude of 10 N. The third damper is then moved away from the first damper to 20% of the cable length. The coefficient c1 equals the coefficient c2 and is chosen to provide the maximum damping ratio of the first mode. Additionally, the position of these two dampers is supposed to

be symmetrical. The resulting curves are displayed in Figures (7) a to c for the first three vibration modes of the cable. In these curves, it is seen that there is an optimal value of c3 / c1 for which the percentage of the decrease of vibrations hits its maximum value. Joining a c3 damping factor higher than this degrades the performance of the third damper.
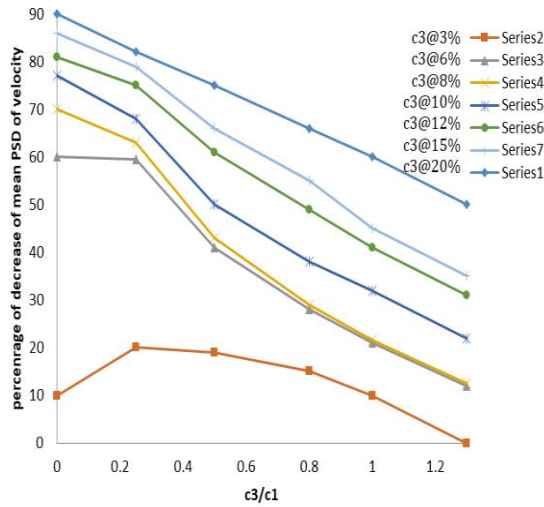
The chosen values for c1 in these curves is as follows.

Rubbber bushings attached to 1% cable length→c1=7700N.s/m
Rubbber bushings attached to 2% cable length→c1=3800N.s/m
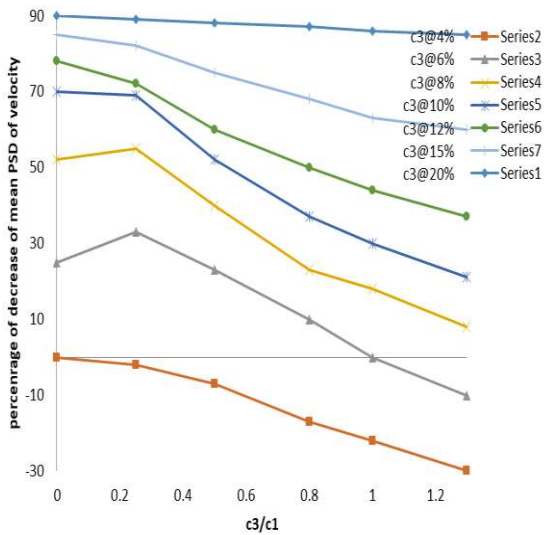Rubbber bushings attached to 3% cable length→c1=2700N.s/m
Rubbber bushings attached to 4% cable length→c1=1900N.s/m
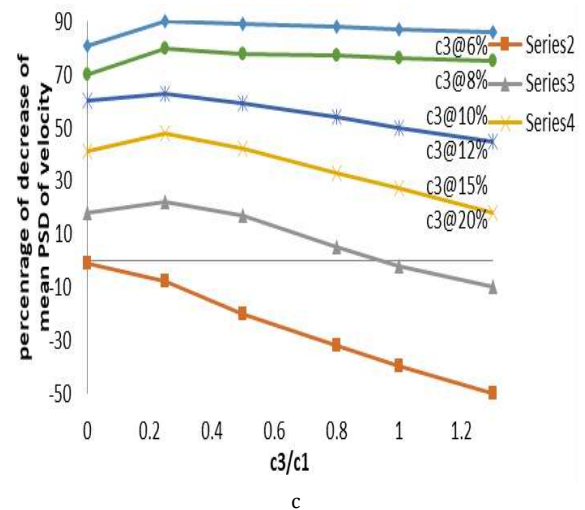Rubbber bushings attached to 5% cable length→c1=1538N.s/m

a

b

c

Figure 7. (a) Diagram of percentage of PSD drop with c3 / c1 in the first mode (spring-damper at 1% of cable length), (b) Diagram of percentage of PSD decrease with c3 / c1 in the second mode (spring-damper at 3% of length) Cable), (c) Diagram of PSD reduction percentage with c3 / c1 in the third mode (spring-damper at 5% cable length)

4. CONCLUSION

In this research, the impact of linear viscous dampers and spring-dampers on decreasing the vibrations of cables, as well as the interaction of these dampers with each other, was studied. Based on the investigation, the subsequent results can be obtained.

Although the induced damping because of the connection of the damper to the end of the cable is minute, owing to the relatively low intrinsic damping of the cable itself, this low damping can further restrict the phenomenon of resonance in the cable. As a result, the amplitude and vibration energy of the cable is noticeably reduced.

If the cable understudy has an insignificant curvature and the amplitude of vibrations is moderate, the nonlinear behavior of the cable can be neglected.

In the case where two viscous dampers or two damper-springers are connected to the cable and the attachment point of these dampers is near enough to the end of the cable, the interaction of the dampers with each other is negligible. As a result, a complete pachecco diagram can still be employed to design them.

If the damping coefficient of the third damper is less than its optimal value, this third damper will further decrease vibrations in the cable. But the resulting damping ratio is less than its maximum value.

In case the damping coefficient of the third damper is greater than its optimum value, this damper may decrease the vibration of the cable. But, by the exceeding of the third damping coefficient of a known value, the total damping ratio decreases compared to the case where only two damper-springs are joined to the cable. That is, by extra increasing the damping coefficient of viscous dampers, its effect on reducing cable vibration becomes negative.

The results of this study can be used to design the required dampers to reduce the vibrations of bridge cables to the extent needed. Although cable structures and suspension bridges are not yet quite popular in Iran, these structures are immediately opening their way in the world owing to various advantages such as high lightness.

Furthermore, as mentioned, linear viscosity dampers can produce optimal damping only in one particular vibration mode, and in other vibration modes, they are harder or softer than their optimal peer. Thus, to obtain maximum damping in several modes, non-linear dampers must be used. Hence, for further research, the nonlinearity of the damper can be factored in.

REFERENCES

1. Çakmak, A. Ş. (1996). Dynamics of structures: theory and applications to earthquake engineering: Prentice Hall, 1995. ISBN 0-13-855214-2, 729 pp. solutions manual (0-13-855231-2).
2. Jayaraman, H. B., & Knudson, W. C. (1981). A curved element for the analysis of cable structures. *Computers & Structures*, *14*(3-4), 325-333.
3. Main, J. A., & Jones, N. P. (2001). Evaluation of viscous dampers for stay-cable vibration mitigation. *Journal of Bridge Engineering*, *6*(6), 385-397.
4. Main, J. A., & Jones, N. P. (2002). Free vibrations of taut cable with attached damper. I: Linear viscous damper. *Journal of Engineering Mechanics*, *128*(10), 1062-1071.
5. Main, J. A., & Jones, N. P. (2003, September). Influence of rubber bushings on stay-cable damper effectiveness. In *Proceedings of Fifth International Symposium on Cable Dynamics* (pp. 15-18).
6. Ni, Y. Q., Ko, J. M., & Zheng, G. (2002). Dynamic analysis of large-diameter sagged cables taking into account flexural rigidity. *Journal of Sound and Vibration*, *257*(2), 301-319.
7. Ozdemir, H. (1979). A finite element approach for cable problems. *International Journal of Solids and Structures*, *15*(5), 427-437.
8. Wang, P. H., Fung, R. F., & Lee, M. J. (1998). Finite element analysis of a three-dimensional underwater cable with time-dependent length. *Journal of sound and vibration*, *209*(2), 223-249.